Original Research Article

TJ | Tumori Journal

Tumori Journal
2023, Vol. 109(3) 314–323

DOI: 10.1177/03008916221110266
journals.sagepub.com/home/tmj


Establishment of 6 pediatric rhabdomyosarcoma patient's derived xenograft models closely recapitulating patients' tumor characteristics

Patrizia Gasparini[1*], Michela Casanova[2*], Giovanni Centonze[3], Cristina Borzi[1], Luca Bergamaschi[2], Paola Collini[4], Adele Testi[5], Stefano Chiaravalli[2], Maura Massimino[2], Gabriella Sozzi[1], Andrea Ferrari[2#] and Massimo Moro[1#]

Abstract

Introduction: The prognosis for patients with metastatic and recurrent pediatric rhabdomyosarcoma (RMS) remains poor. The availability of preclinical models is essential to identify promising treatments We established a series of pediatric RMS patient derived xenografts (PDXs), all faithfully mirroring primary tumor characteristics and representing a unique tool for clarifying the biological processes underlying RMS progression and relapse.

Methods: Fresh tumor samples from 12 RMS patients were implanted subcutaneously in both flanks of immunocompromised mice. PDXs were considered as grafted after accomplishing three passages in mice. Characterization of tumor tissues and models was performed by comparing both morphology and immunoistochemical and fluorescence in situ hybridization (FISH) characteristics.

Results: Six PDXs were established, with a successful take rate of 50%. All models closely mirrored parental tumor characteristics. An increased grafting rate for tumors derived from patients with worse outcome ($p = 0.006$) was detected. For 50% PDXs grafting occurred when the corresponding patient was still alive.

Conclusion: Our findings increase the number of available RMS PDX models and strengthen the role of PDXs as useful preclinical tools for patients with unmet medical needs and to develop personalized therapies.

Keywords

Rhabdomyosarcoma, patient-derived xenografts, personalized therapy

Date received: 11 May 2022; accepted: 12 June 2022

[1]Tumor Genomics Unit, Department of Research, Fondazione IRCCS Istituto Nazionale dei Tumori, Milan, Italy
[2]Paediatric Unit, Fondazione IRCCS Istituto Nazionale dei Tumori, Milano, Italy
[3]First Pathology Division, Department of Pathology and Laboratory Medicine, Fondazione IRCCS Istituto Nazionale dei Tumori di Milano, Milan, Italy
[4]Soft Tissue and Bone Pathology, Histopathology and Pediatric Pathology Unit, Department of Diagnostic Pathology and Laboratory Medicine, Fondazione IRCCS Istituto Nazionale dei Tumori, Milan, Italy
[5]Laboratory of Molecular Pathology, Department of Pathology, Fondazione IRCCS Istituto Nazionale dei Tumori, Milan, Italy

*These authors contributed equally to this work as co-first authors

#These authors contributed equally to this work as co-last authors.

Corresponding author:
Massimo Moro, Tumor Genomic Unit, Department of Research, Fondazione IRCCS Istituto Nazionale dei Tumori, via G. Venezian, Milan, 1, Lombardy 20133, Italy.
Email: massimo.moro@istitutotumori.mi.it

Introduction

Rhabdomyosarcoma (RMS) is the most frequent soft tissue sarcoma of childhood and adolescence: it is a high-grade tumor characterized by local invasiveness and strong propensity to metastasize. RMS shows varying degrees of skeletal muscle differentiation.[1] Two main subtypes are observed in pediatric age: the embryonal RMS (ERMS), characterized by round and spindle cells in a frequent myxoid stroma, often presenting a molecular loss of heterozygosity at 11p15 along with the acquisition of chromosome 8 and several other mutations; and the more aggressive alveolar RMS (ARMS), characterized by a solid growth of round cells, with PAX3/7-FOXO1 fusion genes in the large majority of cases.[2,3] In addition, also sclerosing/spindle cell (Sc/Sp) RMS is reported in pediatric ages, characterized by a variable cellularity, an abundant collagenous stroma and/or spindle cells, and MYOD1 mutations.[1]

Although a large proportion of pediatric RMS patients can currently be cured with intensive multimodal treatments, about 25% patients do not survive due to unresectable, metastatic, or refractory disease. Thus, understanding the biological process of tumorigenesis and exploring the efficacy of new biological drugs still remains an important clinical need in RMS.

Limited appropriate and molecularly well characterized RMS patient-derived pre-clinical models are available. This makes proof-of-concepts preclinical testing of novel molecular targeted compounds a challenge, limiting evidence for *in vivo* preclinical efficacy before going into clinical studies.

Patient-derived xenografts (PDXs) represent *in vivo* models that closely recapitulate many important features of patients' tumors.[4,5] These models have been deeply exploited for studying the biology of the disease, and for developing new treatments. In the last few years, generation of PDXs collections have been reported for many different types of solid tumors.[6–11] PDXs have been widely used to predict therapeutic approaches efficacy,[12–14] and to identify new therapeutic markers[15,16] in adult neoplasia. Their preclinical value has also been consolidated for pediatric malignancies as a panel of 261 PDX models (from 37 distinct tumor entities) have been generated.[17] Moreover in Europe, public-private partnership such as the ITCC-P4 (www.itccp4.eu) project has been launched.

Particularly for RMS PDXs, platforms have been developed and used to predict response for specific treatments.[18–20] Ideally, a PDXs collection should be large enough to encompass heterogeneity of a specific tumor type. Unfortunately, as RMS is a rare tumor, this is hard to achieve and every new model established is considered of great importance as it may offer the possibility to add new critical information necessary to lay foundation for the comprehension of biological processes underlying RMS growth.

For all these reasons, our study was aimed at generating a collection of pediatric RMS of different subtype (ERMS, ARMS, Sc/Sp RMS), clinical presentation, site of onset and stage of disease. We here describe the successful establishment of six RMS PDX derived from patients with different RMS subtypes which recapitulate patients' tumor characteristics.

Materials and methods

Patient selection

All samples were collected from July 2014 to January 2020, with a sterile procedure in the operating room. A diagnosis of RMS and subtyping had been performed on the tumor tissue of the patients following the 2019 WHO Classification of soft tissue and bone tumors (WHO). All ARMS were characterized for the occurrence and type of gene fusion. Sc/Sp RMS was diagnosed on the basis of morphology coupled with the strong and diffuse expression of MyoD1.[1]

Tissue specimens were obtained according to the Internal Review and the Ethics Boards of the Fondazione IRCCS Istituto Nazionale Tumori of Milan. Written informed consent and age-appropriate assent were obtained for all patients. All analyses of clinical and biological data were planned and executed according to the guidelines of the revised Declaration of Helsinki.

PDXs establishment

PDXs were established as previously described.[8,21] PDXs models were propagated for three rounds in mice (P1–P3) before being considered stabilized, and then frozen in a solution of 90% FBS and 10% DMSO and stored in liquid nitrogen. Animal studies were conducted according to the guidelines of the Ethics Committee for Animal Experimentation (OPBA) of the Fondazione IRCCS Istituto Nazionale dei Tumori.[22] All experiments were approved by the OPBA and by the Italian Ministry of Health.

Immunohistochemistry

All tumor samples/tissues and PDX were immunostained for desmin, myogenin, and MyoD1. 2.5/3 micron-thick sections were cut from paraffin blocks, dried, de-waxed, rehydrated, and unmasked (with Dako PT-link, EnVision™ FLEX Target Retrieval Solution, High pH 96°C). Antibodies agains desmin (clone D33, Dako - Agilent, dilution 1:400), myogenin (clone F5D, Dako - Agilent, Ready-to-Use) and MyoD1 (clone 5.8A, Dako - Agilent, dilution 1:50) were incubated with a commercially available detection kit (EnVision™ FLEX+, Dako, Agilent) in an automated Immunostainer (Dako Autostainer Link 48 - Agilent)

PAX3/7-FOXO1 assessment by fluorescence in situ hybridization (FISH) analysis

FISH analysis was performed on selected areas on 2–4 μm-thick paraffin sections of all Formalin-Fixed Paraffin-Embedded (FFPE) ARMS human and PDX's tissues by counting at least 100 tumor cells, Briefly, a commercial available dual color single fusion probe (Abbott Molecular, Zyto*Light* ® SPEC FOXO1/PAX7 Dual Color Single Fusion Probe), specifically designed to detect the translocation t(1;13) (p36.1;q14.1) was used to corroborate the diagnosis of PAX7/FOXO1 fusion transcript. The commercial probe was used according to manufacturer's instructions. Interpretation of FISH results in a normal situation without a translocation involving the respective gene regions, revealed two separate green (distal to the PAX7 breakpoint region) and orange signals appear (proximal to the FOXO1 breakpoint region). Whereas, in presence of a rearrangement, the gene fusion was indicated by one orange/green fusion signal, together with one separate orange signal, one separate green signal.

Statistical analysis

Analyses were performed using GraphPad Prism (GraphPad Software, La Jolla California USA) and R software i386 3.6.3 (packages: ggplot2, ggpubr, ggsci, survival and survminer) and RStudio Version 1.2.5033.

Results

Establishment of a pediatric patient derived xenografts perpetual bank

Tumor samples from 12 RMS patients (five ARMS, five ERMS, and two Sc/Sp RMS; 1-23 years old) have been implanted in both flanks of SCID mice. PDXs showed variable growth features during the first three passages (P1–P3). In particular in the P1-P3 period latency time was generally higher and variable, with tumor volume increasing and decreasing, whereas at P3 PDXs grew with more homogeneous characteristics (Suppl. Figure 1A-C). PDXs were considered as grafted after reaching P3. We successfully generated six RMS PDXs (two ARMS, three ERMS, and one Sc/Sp RMS), reaching 50% (6/12) take rate (40%, 60%, and 50% within ARMS, ERMS, Sc/Sp RMS, respectively). We reached 67% (2/3) take rate for fusion-positive ARMS, whereas fusion-negative ARMS, both derived from paratesticular tumors, did not graft as PDXs (Table 1).

PDXs mirror the most important human tumor features

ARMS and ERMS subgroups were maintained in all the successfully grafted PDXs (Table 2). ERMS PDXs were characterized by mostly spindle-shaped cells in a fibrous or fibromyxoid stroma, with reactivity for both desmin and myogenin, and ARMS models were characterized by mostly round cells with a high reactivity for both markers (Figure 1). One of the established PDX (PT2) was derived from a tumor diagnosed as a translocated ARMS with PAX7/FOXO1 fusion by RT-qPCR analysis. FISH analysis performed on tumor and corresponding PDX samples showed a similar FOXO1 amplification (FOXO1X8~>15, and FOXO1X3>15 in tumor and PDX, respectively), and few signals indicating PAX7/FOXO1 fusion (12 and 10% of cells with one fusion signal in tumor and PDX, respectively, Figure 1B). PAX7/FOXO1 translocation was confirmed both in the human tumor and in the PDXs by NGS analysis (data not shown). Of note, PT3 was derived from a tumor (RMS2) diagnosed as Sc/Sp RMS, and characterized by areas with different density of cells (Figure 2). In the PDX, a central core of rhabdomyoblastic cells was surrounded by densely cellular spindle cells. Both human tumor and the corresponding PDX showed a strong and diffuse nuclear immunoreactivity for MyoD1 (Figure 2).

PDX grafting is associated with tumor aggressiveness

As shown in Table 1, tumor samples of patients with dismal clinical outcome revealed increased graft capability compared to those derived from patients with a longer survival. We experienced a successful PDX graft in 100% (5/5) of tumors derived from patients with fatal prognosis, and 14.3% (1/7) of tumors derived from patients who were still alive at the time of the analysis ($p = 0.015$, Table 1). The Kaplan-Meier estimate showed a poorer prognosis for patients whose tumor successfully grafted in mice (log rank $p = 0.006$, Figure 3). A worse prognosis was observed for tumors with IRS IV (log rank $p = 0.01$, Suppl. Figure 3A), whereas no significant difference in overall survival (OS) were observed between patients in pediatric (0-14 years old) and adolescent (15-23 years old) age (log rank $p = 0.38$, Suppl. Figure 3B). PDXs take remained a negative prognostic marker also within tumors categorized as IRS group I-III (log rank $p = 0.02$, Suppl. Figure 3C).

PDXs as avatars to develop personalized therapies

The median grafting time (days between tumor injection and PDX graft) was 195 days, while the fastest and the slowest PDXs had a grafting time of 165 and 315 days, respectively (Suppl. Table 1). RMS PDXs were subdived into three groups according to their growth characteristics at P_3 (lag time – LT, and exponential growth time - EGT, Suppl. Table 1). Group I PDXs (PT9 and PT14) were characterized by a short (15-20 days) LT and a long (35-45 days) EGT. PDXs belonging to Group II (PT2, PT3, and

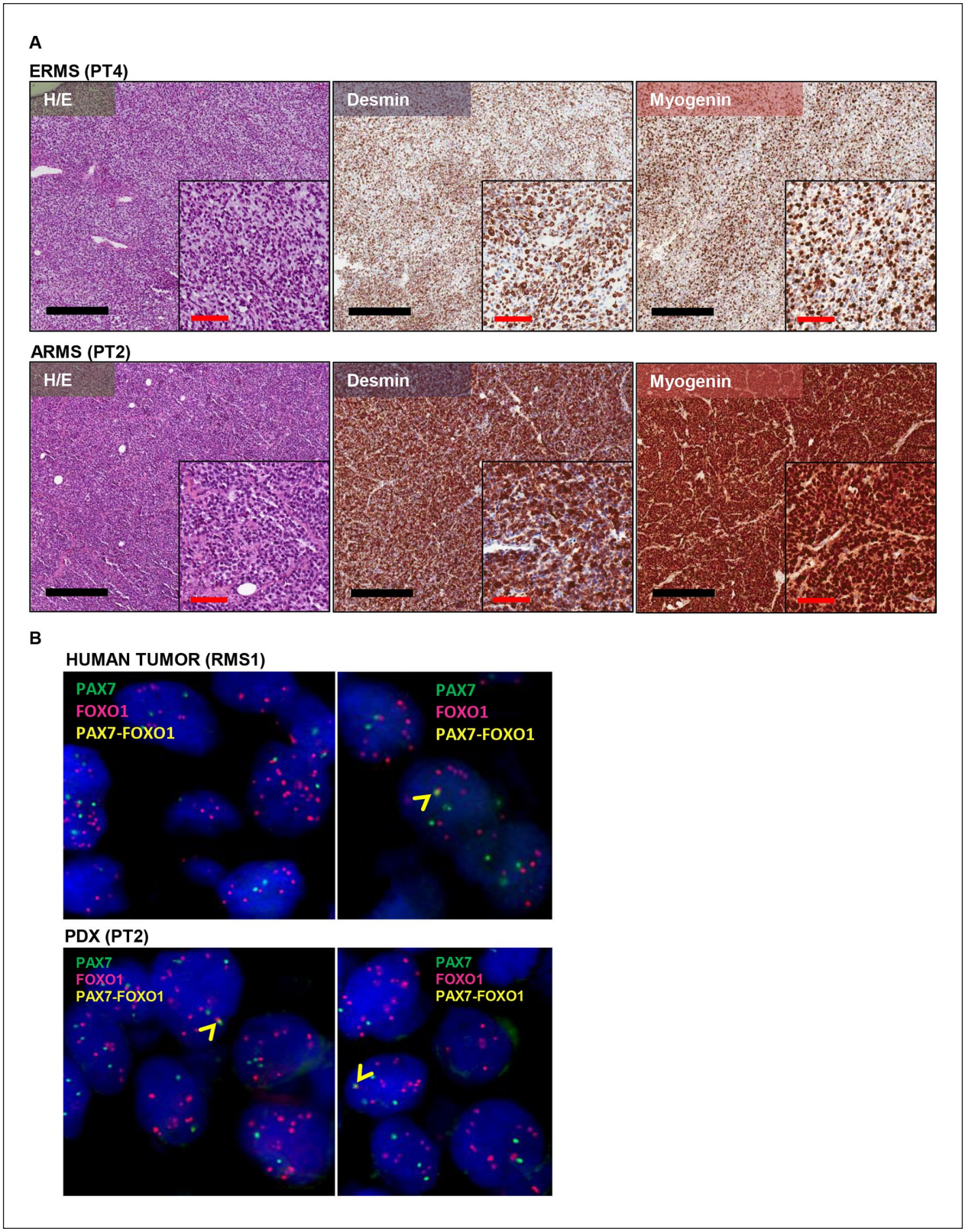

Figure 1. (A) Representative images of RMS PDX morphology and immunohistochemical analysis. PDXs morphological and immunophenotypical features of ERMS and ARMS are depicted in H/E staining. Black line: 400 μm; red line= 100 μm; (B) FISH analysis showing amplification of FOXO1 gene and PAX7/FOXO1 fusion product in RMS1 human sample and in the corresponding PDX (PT2). *Blue: nuclei, red: FOXO1 gene, green: PAX7 gene, yellow: PAX7/FOXO1 fusion gene.*

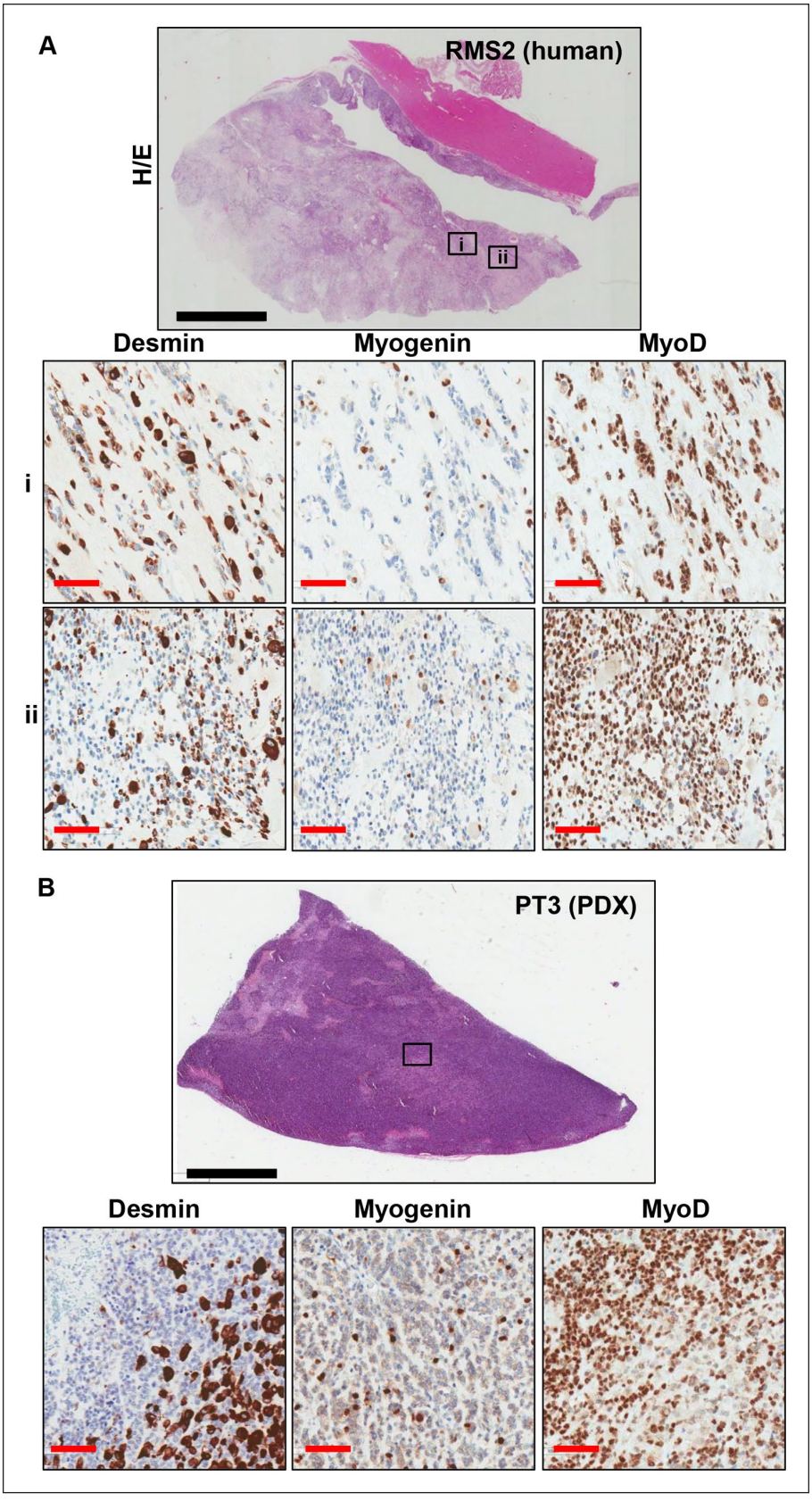

Figure 2. Representative IHC images of Desmin, Myogenin and MyoD1 staining on human (*A*) and PDX (*B*) tissue sections. (A) In the human tumor, two differently cellulated areas are appreciable, the first poorly cellulated and the second densely cellulated (ii). (B) In the PDX only the densely cellulated component was detected. Black line: 6mm; red line= 100 μm.

Table 1. Patients and tumors characteristics, overall and according to graft.

		Graft		
	All subjects (n=12)	Yes (n=6)	No (n=6)	p-value
Patients characteristics				
Sex				
Female	3 (25.0)	1 (33.3)	2 (66.7)	*1.000*[1]
Male	9 (75.0)	5 (55.5)	4 (44.5)	
Age				
Mean (SD) – Median (IQR)	14.0 (6.0) – 14.0 (11.8-17.0)	12.9 (5.9) – 13.0 (11.0-16.0)	15.8 (5.1) – 15.5 (13.5-20.3)	
Paediatric (0-14 years old)	7 (58.3)	5 (71.4)	2 (28.6)	
Adolescent (15-25 years old)	5 (41.7)	1 (20.0)	4 (80.0)	*0.242*[1]
Outcome				
Mortality				
Alive	7 (58.3)	1 (14.3)	6 (85.7)	***0.015***[1]
Dead	5 (41.7)	5 (100)	0 (0.0)	
Tumor characteristics				
IRS				
I/II	4 (33.3)	1 (25.0)	3 (75.0)	
III/IV	8 (66.7)	5 (62.5)	3 (37.5)	*0.546*[1]
I/II/III	10 (83.3)	6 (60.0)	4 (40.0)	
IV	2 (16.7)	0 (0.0)	2 (100)	*0.455*[1]
TNM				
T = 1	5	1	4	
T > 1	7	5	2	*0.242*
N = 0	10	4	6	
N > 0	2	2	0	0.455
Subtype				
ERMS	7 (58.9)	4 (57.1)	3 (42.9)	*1.000*[1]
ARMS	5 (41.1)	2 (40.0)	3 (60.0)	
PAX3-7/FKHR+	*3 (60.0)*	*2 (66.7)*	*1 (33.3)*	*0.400*[1]
PAX3-7/FKHR-	*2 (40.0)*	*0 (0)*	*2 (100)*	
Tumor Site				
ERMS	7 (58.9)			
Paratesticular	*1 (14.3)*	*0 (0.0)*	*1 (100.0)*	
Limb	*2 (28.6)*	*1 (50.0)*	*1 (50.0)*	
Prostate	*1 (14.3)*	*1 (100.0)*	*0 (0.0)*	
Trunk	*2 (28.6)*	*1 (50.0)*	*1 (50.0)*	
Abdomen	*1 (14.3)*	*1 (100.0)*	*0 (0.0)*	
ARMS	5 (41.1)			
Paratesticular[2]	*2 (40.0)*	*0 (0.0)*	*2 (100.0)*	
Limb	*3 (60.0)*	*2 (66.7)*	*1 (33.3)*	

[1]Two-tailed Fisher's exact test; [2]both fusion-negative. ARMS: alveolar rhabdomyosarcoma ERMS: embryonal rhabdomyosarcoma; IQR: interquartile range; IRS: intergroup rhabdomyosarcoma studies; SD: standard deviation.

Table 2. Comparison between human tumor and PDX diagnosis.

Human		PDX	
ID	*Diagnosis*	*Diagnosis*	*ID*
RMS1	ARMS	ARMS	PT2
RMS2	ERMS	ERMS	PT3
RMS3	ERMS	ERMS	PT4
RMS6	ERMS	ERMS	PT9
RMS9	ARMS	ARMS	PT13
RMS10	ERMS	ERMS	PT14

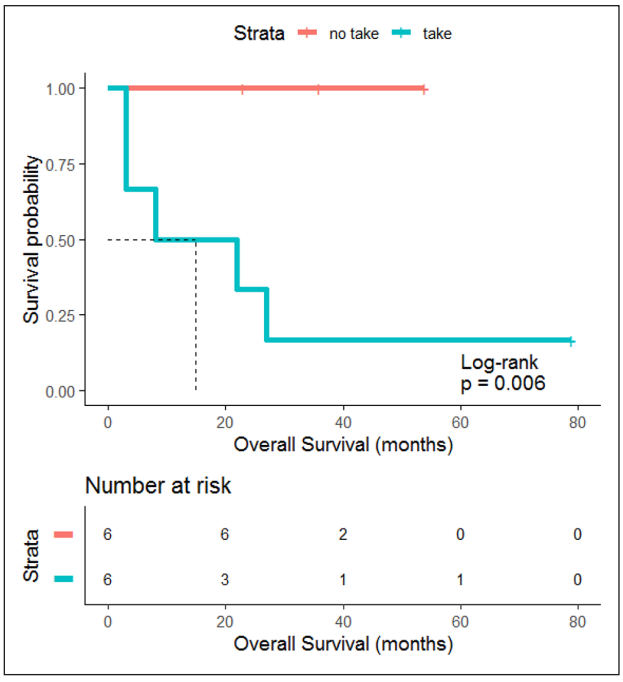

Figure 3. Prognostic significance of PDX graft. Kaplan Meier estimate shows that patients whose tumor successfully grafted in mice had a significantly lower OS compared to those whose tumors did not grow as PDX (p=0.006).

PT4) showed a long LT (35-45 days) and a shorter EGT (25-30 days). PT13 was characterized by a slow growth with long LT (55 days) and long EGT (50 days, Figure 4A, B and Suppl. Table 1). Changes in growth characteristics were mainly ascribed to a different lag time (Figure 4B). No significant correlation between growth characteristics in mouse and tumor subtype or patients OS was observed (Suppl. Figure 4). Of note, patients OS was higher than $P_{1\text{-}4}$ time for 50% of grafted PDXs (Figure 4C).

Discussion

An established collection of six pediatric RMS PDXs, with a 50% graft rate was here reported and described. The grafted models recapitulate the main clinical and pathological features of the tumor of origin. Indeed, morphology, and immunophenotype were maintained in the mouse models. Thus, RMS PDXs could represent *in vivo* models valuable for studying RMS biology, and potentially useful for testing new therapies. The analysis of clinico-pathological characteristics indicated a strong correlation between PDX establishment and patients OS, as already reported in another pediatric sarcomas platform.[23] Indeed, grafted PDXs were derived mainly from patients with very aggressive tumors. We observed a higher take rate for fusion-positive ARMS compared to ERMS, further suggesting that a more aggressive RMS histology is more likely to successfully grow in mice. Moreover, two fusion-negative paratesticular ARMS, already proposed as a RMS with favorable prognosis,[24,25] did not give rise to PDXs. Interestingly, the prognostic role of PDX graft was maintained also for IRS group I-III tumors, indicating that PDX graft may potentially be considered as prognostic also for low stage RMS. These insights further highlight the importance for RMS PDX as a pre-clinical model for testing new therapies, particularly so in case of aggressive RMS, with no effective therapy.

Tumor aggressiveness is often associated to the capacity of cancer cells to disseminate and to grow as metastasis in distant organs. RMS PDXs described in our study are human tumors that grow subcutaneously in mice. Thus, the correlation between OS and PDX grafting may indicate that only RMS more proficient in developing metastasis are able to grow successfully in the "distant organ" represented by the mice subcutaneous region. Moreover, differences in PDXs growth rate are mainly due to increased lag time, which reflects the capability of tumor cells to establish a pro-tumorigenic cross-talk with murine tumor microenvironment (TME), reported to influence tumor growth as well as metastasis formation.[26–28] Based on this consideration, RMS PDXs may also represent a useful model to study mechanisms underlying metastasis development.

Interestingly, we reported histological differences in one PDX (PT3) compared to the corresponding human tumor (RMS2). Indeed, in PDX only the most cellular component was observed. Of note, MyoD1-positivity of cells was maintained in the murine model. MyoD1 expression was reported as associated with a dismal prognosis in RMS.[29] We recently reported the correlation between tumor aggressiveness and PDX graft, and the loss of less aggressive histological subtypes in lung cancer PDXs.[8] Similarly, in this study we encounter the same association of tumor aggressiveness in graft rate of pediatric RMS PDXs. Thus, another hypothesis to explain morphological differences between RMS2 and PT3 may be that only the more aggressive cells survived implantation in mice.

In conclusion, we here report the establishment of a small RMS PDXs platform, that closely recapitulates primary tumors features in terms of morphology, and immunphenotype. Despite the limited number of PDXs, we showed that tumor graft was directly related to RMS aggressiveness, further strengthening the importance of these models. Our data are the proof-of-concept that the effort to develop *in vivo* model is a fruitful investment also in the case of rare tumors such as RMS. However, the limited size of RMS cases available each year in a single institute makes it almost impossible to establish a complete PDX platform, comprehensive of all genetic alterations involved in RMS development.[30] For this reason, it is of critical important to achieve a multicentric effort to join resources and expertise like that by the European Innovative Medicine Initiative (IMI2) to develop a

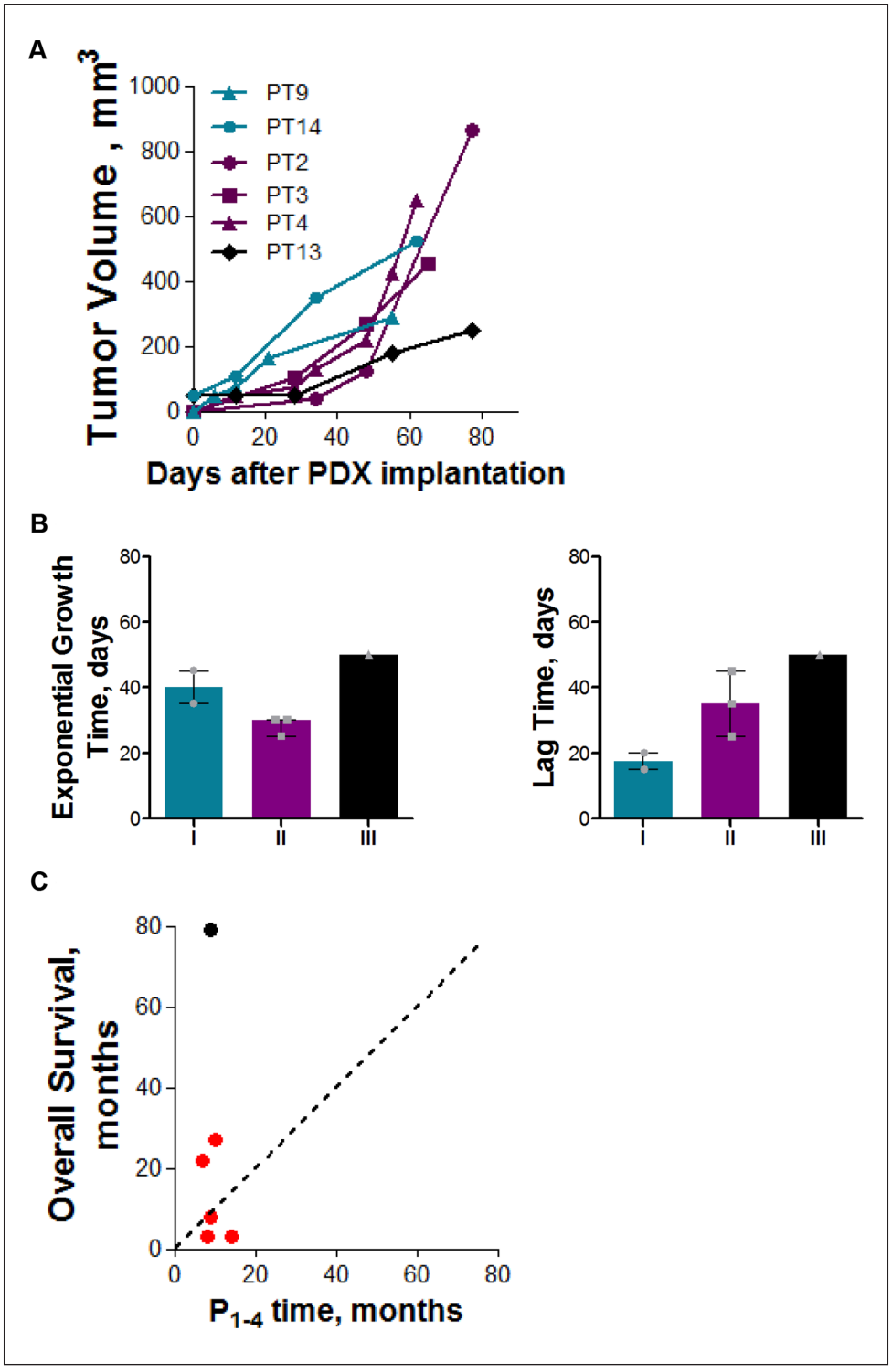

Figure 4. (A) PDX growth curves. Graph shows the growth of all successfully implanted PDX at P3. In blue are indicated models belonging to group I (low latency period and slow growth), in violet those belonging to group II (high latency period and fast growth), and in black the PDX belonging to group III (high latency period and slow growth); (B) different growth characteristic in terms of latency period and exponential growth time of the three identified PDXs groups; (C) Comparison between the time needed for the PDX to accomplish four passages in mice and the OS of the corresponding patient. Dotted line indicate x=y line, red = dead; black = no evidence of disease.

pediatric preclinical platform (ITCCP4 - https://www.itccp4.eu/). Nowadays, great efforts are focused at the generation of representative and robust preclinical models (PDXs, genetically engineered mouse models –GEMMs- and organoids) accurately reflecting human disease and providing efficient platforms for *in vivo* functional new drugs that would significantly accelerate the development of more precise and efficacious drugs for children with malignant solid tumors. Children have been given drugs designed for adults although malignancies in children are fundamentally different from their adult equivalents. In particular, the PDX platforms represent an unprecedented effort for an extensive molecular characterization and preclinical utilization of pediatric solid tumor models aiming to overcome the gaps in drugs provided to children and to deliver more precisely tailored therapies for children.

Author's contributions

PG, MC, LB, SC, AF, and MMo created the experimental design; PG, GC, CB, PC, AT, and M.Mo acquired and analysed the data. PG, MC, GC, CB, LB, PC, AT, SC, MMa, GS, AF, MMo participated in data interpretation, as well as in writing and editing the manuscript. All authors approved the final version of the manuscript.

Declaration of conflicting interests

The author(s) declared no potential conflicts of interest with respect to the research, authorship, and/or publication of this article.

Funding

The author(s) disclosed receipt of the following financial support for the research, authorship, and/or publication of this article: The study was supported by Associazione Bianca Garavaglia: A/15/01N, A/18/01A,

ORCID iDs

Patrizia Gasparini https://orcid.org/0000-0002-9548-3724
Cristina Borzi https://orcid.org/0000-0003-2850-6559
Andrea Ferrari https://orcid.org/0000-0002-4724-0517
Massimo Moro https://orcid.org/0000-0003-2562-4007

Supplemental material

Supplemental material for this article is available online.

References

1. World Health Organization. WHO Classification of Tumors – 5th edition – Soft tissue and bone tumors. Book, edited by WHO Classification of Tumors Editorial Board, 2020, p.472–474.
2. Chen X, Stewart E, Shelat AA, et al. Targeting oxidative stress in embryonal rhabdomyosarcoma. *Cancer Cell* 2013; 24: 710–724.
3. Shern JF, Chen L, Chmielecki J, et al. Comprehensive genomic analysis of rhabdomyosarcoma reveals a landscape of alterations affecting a common genetic axis in fusion-positive and fusion-negative tumors. *Cancer Discov* 2014; 4: 216–231.
4. Woo X, Giordano J, Srivastava A, et al. Author Correction: Conservation of copy number profiles during engraftment and passaging of patient-derived cancer xenografts. *Nat Genet* 2021; 53: 761.
5. Rizzo G, Bertotti A, Leto S, et al. Patient-derived tumor models: a more suitable tool for pre-clinical studies in colorectal cancer. *J Exp Clin Cancer Res* 2021; 40: 178–195.
6. Fichtner I, Rolff J, Soong R, et al. Establishment of patient-derived non-small cell lung cancer xenografts as models for the identification of predictive biomarkers. *Clin Cancer Res* 2008; 14: 6456–6468.
7. Rivera M, Fichtner I, Wulf-Goldenberg A, et al. Patient-derived xenograft (PDX) models of colorectal carcinoma (CRC) as a platform for chemosensitivity and biomarker analysis in personalized medicine. *Neoplasia* 2021; 23: 21–35.
8. Moro M, Bertolini G, Caserini R, et al. Establishment of patient derived xenografts as functional testing of lung cancer aggressiveness. *Sci Rep* 2017; 7: 6689–6700.
9. Wu Y, Wang J, Zheng X, et al. Establishment and preclinical therapy of patient-derived hepatocellular carcinoma xenograft model. *Immunol Lett* 2020; 223: 33–43.
10. Coussy F, de Koning L, Lavigne M, et al. A large collection of integrated genomically characterized patient-derived xenografts highlighting the heterogeneity of triple-negative breast cancer. *Int J Cancer* 2019; 145: 1902–1912.
11. Conte N, Mason J, Halmagyi C, et al. PDX Finder: A portal for patient-derived tumor xenograft model discovery. *Nucleic Acids Res* 2019; 47: D1073–1079.
12. Moro M, Caiola E, Ganzinelli M, et al. Metformin enhances cisplatin-induced apoptosis and prevents resistance to cisplatin in co-mutated KRAS/LKB1 non-small cell lung cancer (NSCLC). *J Thorac Oncol* 2018; 13: 1692–1704.
13. Hunter A, Newman H, DeZern A, et al. Integrated human and murine clinical study establishes clinical efficacy of ruxolitinib in chronic myelomonocytic leukemia. *Clin Cancer Res* 2021; Epub 2021 July 12 doi: 10.1158/1078-0432.CCR-21-0935.
14. Vangala D, Ladigan S, Liffers S, et al. Secondary resistance to anti-EGFR therapy by transcriptional reprogramming in patient-derived colorectal cancer models. *Genome Med* 2021; 13: 116.
15. Bertotti A, Migliardi G, Galimi F, et al. A molecularly annotated platform of patient- derived xenografts ("xenopatients") identifies HER2 as an effective therapeutic target in cetuximab-resistant colorectal cancer. *Cancer Discov* 2011; 1: 508–523.
16. Renuse S, Madamsetty V, Mun D, et al. Tyrosine phosphoproteomics of patient-derived xenografts reveals ephrin type-b receptor 4 tyrosine kinase as a therapeutic target in pancreatic cancer. *Cancers (Basel)* 2021; 13: 3404.
17. Rokita JL, Rathi KS, Cardenas MF, et al. genomic profiling of childhood tumor patient-derived xenograft models to enable rational clinical trial design. *Cell Rep* 2019; 29: 1675-1689.e9.
18. Manzella G, Schreck LD, Breunis WB, et al. Phenotypic profiling with a living biobank of primary rhabdomyosar-

coma unravels disease heterogeneity and AKT sensitivity. *Nat Commun* 2020; 11: 1–15.
19. Hooper JE, Cantor EL, Ehlen MS, et al. A patient-derived xenograft model of parameningeal embryonal rhabdomyosarcoma for preclinical studies. *Sarcoma* 2015; 2015: Article ID 826124, 7 pages.
20. Cramer S, Miller A, Pressey J, et al. Pediatric anaplastic embryonal rhabdomyosarcoma: targeted therapy guided by genetic analysis and a patient-derived xenograft study. *Front Oncol* 2018; 7: 327–332.
21. Moro M, Bertolini G, Tortoreto M, et al. Patient-derived xenografts of non small cell lung cancer: Resurgence of an old model for investigation of modern concepts of tailored therapy and cancer stem cells. *J Biomed Biotechnol* 2012; 2012: Article ID 568567, 11 pages.
22. Workman P, Aboagye EO, Balkwill F, et al. Guidelines for the welfare and use of animals in cancer research. *Br J Cancer* 2010; 102: 1555–1577.
23. Castillo-Ecija H, Pascual-Pasto G, Perez-Jaume S, et al. Prognostic value of patient-derived xenograft engraftment in pediatric sarcomas. *J Pathol Clin Res* 2021; 7: 338–349.
24. Dantonello TM, Vokuhl C, Scheer M, et al. Paratesticular alveolar rhabdomyosarcomas do not harbor typical translocations: a distinct entity with favorable prognosis? *Virchows Arch* 2018; 472: 441–449.
25. Ferrari A, Bisogno G, Casanova M, et al. Is alveolar histotype a prognostic factor in paratesticular rhabdomyosarcoma? The experience of Italian and German Soft Tissue Sarcoma Cooperative Group. *Pediatr Blood Cancer* 2004; 42: 134–138.
26. Kalluri R. The biology and function of fibroblasts in cancer. *Nat Rev Cancer* 2016, p. 582–98.
27. Hanahan D and Weinberg RA. Hallmarks of cancer: The next generation. *Cell* 2011; 144: 646–674.
28. Quail DF and Joyce JA. Microenvironmental regulation of tumor progression and metastasis. *Nat Med* 2013; 19: 1423–1437.
29. Shern JF, Selfe J, Izquierdo E, et al. Genomic classification and clinical outcome in rhabdomyosarcoma: A report From an International Consortium. *J Clin Oncol* 2021; 39: 2859–2871.
30. Ferrari A, Gasparini P and Casanova M. A home run for rhabdomyosarcoma after 30 years: What now? *Tumori* 2020; 106: 5–11.